Planing Hull Performance Evaluation Using a General Purpose CFD Code

Eric Thornhill[1], Neil Bose[1], Brian Veitch[1], Pengfei Liu[2]
([1]Memorial University of Newfoundland, [2]National Research Council – Institute for Marine Dynamics)

ABSTRACT

Model experiments were used to evaluate CFD simulations of a high-speed planing vessel. Fluent (v5.3) was used to simulate the flow around a planing vessel at steady speed through calm water using 3D unstructured hybrid grids with hanging node refinement. Force and moment data from the simulations were used in an iterative scheme to determine the dynamic equilibrium position of the model at selected speeds. The numerical results are compared with experimental data from model tests. The strengths and weaknesses of the numerical approach are discussed.

INTRODUCTION

Performance prediction is an important part of vessel design. Common methods for predicting planing hull performance include using empirical equations and model testing. Empirical equations are often only applicable to similar hull types over a small range of parameters, while model testing is often prohibitively expensive, particularly for small craft. Ever increasing computer power is making the use of computational fluid dynamics (CFD) as a performance prediction tool a practical alternative. This paper presents the results of a study to use CFD to evaluate the performance of a high-speed planing vessel moving at steady speed through calm water.

After a review of the state-of-the-art in CFD methods (Thornhill, 2002), it was decided that an unstructured, multiphase, finite volume code employing the volume-of-fluid (VOF) method for free surface capturing would be used for the study. The use of a commercial CFD code was found to be the best alternative as they are publicly available, generally undergo extensive validation, have a wide user-base, and receive periodic upgrades and improvements. The code chosen was Fluent (v5.3).

Fluent could not, however, be used to directly simulate the behaviour of a planing vessel. The performance of a high-speed vessel is intimately linked to the orientation of the hull at speed, which cannot be known *a priori*. Planing hulls rise and change trim angle in response to the pressure field generated by the flow. In order to solve for these changes in hull position, the simulation method had to ensure that dynamic equilibrium was achieved in terms of lift and trimming moment. This was accomplished with an iterative scheme wherein the flow field was solved for discrete hull orientations that were then adjusted based on force and moment results until the conditions of equilibrium were met.

The work began with a set of physical model experiments to provide the baseline to which the numerical results could be compared. Three sets of simulations were then performed to evaluate the prediction method. The first set fixed the hull orientation to match the trim and vertical position measured in the physical experiments. This was executed to provide a direct comparison of the numerical results to the physical results. A second set of simulations was then performed where only the equilibrium condition of lift was satisfied. Trim angles remained fixed at the experimental values. These were used to examine the influence of sinkage on the results. The last set of simulations solved for equilibrium in both lift and trimming moment and represent the results of predictions that would be produced without the benefit of physical experiments.

A brief description of the physical model experiments is given, followed by a description of the numerical approach. Results of the simulations are then given along with a discussion, and a comparison with the physical model results.

BACKGROUND

Savitsky (1964) discussed the basic hydrodynamic characteristics of prismatic planing hulls. Based on previously published work, empirical equations for lift, drag, wetted area, center of pressure, and porpoising limits as functions of speed, trim angle,

configurations (displacement and longitudinal center of gravity) over a range of speeds. Measurements were made of tow force, running trim and sinkage, hull pressures, wetted lengths and surface area, as well as detailed wave profiles. Additional tests were done to measure the boundary layer profiles at two locations along the hull using a laser Doppler velocimeter.

The planing hull used was a 1:8 scale model of a full scale vessel currently in operation. The hull surface, shown in Figure 1, was marked with station numbers on the bottom and port side. Knife edges extending 1mm from the hull surface were fitted along the chines to promote flow separation. The hull was not prismatic but did have a simple shape as shown in Figure 2. This cross section was constant from the transom for about 2/3 the length of the hull. A small flat bottom area at the centerline turns to a low deadrise of 5.9°. This deadrise then turns sharply to 40.8° near the chine (see Figure 2).

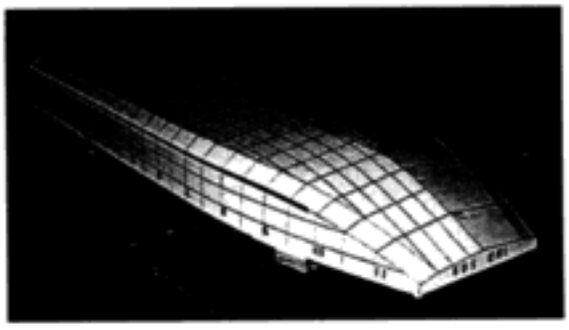

Figure 1: Model Hull (LOA = 1.475m).

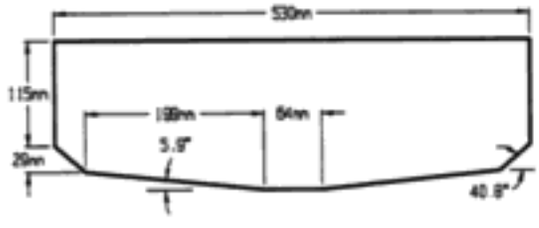

Figure 2: Model Hull Cross Section.

The model was free to heave, pitch and roll but was restrained in yaw. The tow point was located 22 cm forward from the transom and 5 cm above the baseline. Although several ballast conditions were tested, only the design ballast condition was examined in the numerical simulations. This condition consisted of a model displacement of 29.6 kg with a center of gravity located 53.4 cm from the transom, and 2.6 cm above the baseline. Resting draft at the tow point measured 6.7 cm with a bow-up trim angle of 1.1°. The model was tested for speeds at intervals of 0.5 m/s up to 7.0 m/s.

NUMERICAL APPROACH

The Fluent (v5.3) CFD software is a finite volume code using the VOF method for free surface capturing. It includes several turbulence models and supports fully unstructured hybrid adaptive meshes. Though later used to solve for the dynamic equilibrium position of the hull at speed, the code was first tested to see if it could simulate the flow around a planing hull in general.

During this testing phase, combinations of domain sizes, meshing strategies, and solver parameters were examined, many of which created divergent solutions. The following are some of the conclusions from this study:

- Although the problem was of a steady-state flow, a transient solution scheme was necessary.
- Time steps needed to be very small to avoid divergence (~0.001 seconds).
- The solution had to progress for some time in order for pressure-induced forces to stabilize (~2500 time steps). Figure 3 shows an example of lift force history of a typical simulation.
- Turbulence models such as the Spallart-Allmaras and k-ε models could not be used in their standard forms as they created excessive turbulence generation at the air/water interface on the hull bottom that quickly led to divergence.
- When using an unstructured mesh that does not have element faces that coincide with the calm water surface (i.e. elements sporadically crossed the initial air/water boundary), care had to be taken to ensure these elements were assigned the correct volume fraction when initializing for the first iteration.

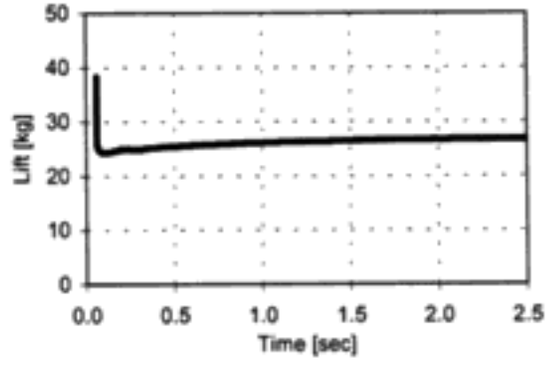

Figure 3: Lift Force History

deadrise angle and loading were given. A procedure was presented for using these equations to predict the performance of a prismatic planing hull. This paper, and the work it was derived from, presents one of the earliest methods for predicting planing hull performance and is still widely used today. This iterative method was based on choosing trim angles, which were then fed into empirical equations that produced values for lift and moment. Iterations continued until these values balanced those produced by the hull's weight and center of gravity.

Ikeda et al. (1993) addressed the need to include the effects of trim and sinkage in high speed craft predictions by performing a set of captive model tests with systematic variations of the model's position and attitude. Nine model shapes were tested. The model was fixed to the tow carriage by a three-component dynamometer that measured lift, drag and trimming moment. Sinkage and trim were incrementally varied to create a database of the hydrodynamic forces for each model over a range of Froude numbers. A computer program was also developed to use this database to estimate the sinkage, trim angle, and resistance of a given model at speed for a given ballast condition (displacement and LCG). Hydrodynamic forces could be determined by interpolation from the database for a given vessel attitude in an iterative scheme until they were in equilibrium with the model's weight and LCG. Simulations of this type were found to be in good agreement with results obtained from free-attitude model tests.

Brizzolara et al. (1998) presented comparisons of wave patterns and wave resistance from both numerical and experimental results. A high speed monohull and two catamaran type hulls were used in model tests at Froude numbers up to 0.9. Their boundary element code, previously used for slower speed vessels, was extended for use on high speed vessels by including calculations of dynamic equilibrium. Forces and moments were evaluated after each iteration and the model's position was updated and re-meshed. The cycle continued until convergence was achieved (usually under 10 iterations). Results for the Wigley hull in the speed range from 0.2 to 0.8 were shown to be under-predicted for sinkage, trim, and wave resistance, though trends in the data were roughly followed.

Yang et al. (2000) extended their unstructured, free surface, inviscid, finite element based flow solver (see Löhner et al., 1998) to account for sinkage and trim effects in steady ship flows. Simulations began with the model in its "at-rest" position. The flow solution was then calculated and used to determine sinkage and heave corrections for the next iteration. The near field mesh moved with the hull, far field meshes remained fixed, while intermediate mesh elements were smoothed for even transition from the near to far field grids. Iterations continued until dynamic equilibrium was achieved. Sinkage and trim corrections at each iteration were based on current flow results in conjunction with the vessel's waterplane area and moment of inertia. Tests were performed for the Wigley and Series 60 hulls over a range of Froude numbers. Results indicated significant differences in wave drag between fixed and free to trim and sink configurations, in agreement with experimental observations.

Subramani et al. (2000) extended a CFD code (CFDSHIP-IOWA) for surface-ship boundary layers, wakes and wave fields to include the capability of predicting sinkage and trim. Simulations were performed on hulls of the naval combatant FF1052 and the Series 60. The CFD code uses the finite volume method for block-structured grids. It employed the Baldwin-Lomax turbulence model and accounted for the free surface boundary conditions with the aid of a body-free-surface conforming grid. Dynamic trim and sinkage were calculated iteratively. Forces and moments on the hull were summed at the end of each iteration. The hull was then re-positioned and the domain grid regenerated for the next iteration, or until equilibrium was achieved. Simulations on the two hulls used mesh sizes from 216,000 to 906,000 nodes. When compared with model experimental data, it was found that although the trends in sinkage and trim were predicted correctly, the percentage difference in absolute values varied with Froude number.

The importance of dynamic equilibrium calculations in vessel performance prediction has been addressed by all of the above authors. The procedure was similar in all cases. Different hull orientations were tested in an iterative scheme until forces and moments matched the required values. Planing vessel performance is the most sensitive to hull orientation making the additional equilibrium calculations essential. This problem was addressed in the current work by using a similar iterative technique. A low dead-rise planing hull was chosen (more conventional hull shapes were used by Yang et al. 2000, and Subramani et al. 2000). Simulations were performed using a RANS CFD code with a free surface capturing method.

PHYSICAL MODEL TESTS

The physical model experiments were performed in the Clearwater Towing Tank at the National Research Council of Canada's Institute for Marine Dynamics and consisted of a series of resistance tests with a planing craft. Tests covered several ballast

One of the consequences of these conclusions was that it was necessary to restrict the mesh size as much as possible in order to keep computation times reasonable due to the large number of small time steps required. The final meshing strategy that was used, relied on a relatively small domain size initially given a fairly coarse mesh. The elements within 20 cm of the hull (model scale) were then subject to hanging node refinement, resulting in increased resolution in this area. Mesh sizes produced from this process ranged in size from approximately 125,000 to 150,000 elements. Solution time on a 500au DIGITAL Personal Workstation took from 2 to 4 days for a single simulation.

The planing model domain, shown in Figure 4, was defined by a box (referred to as a 'tank') 5.5 m long, 1.6 m wide and 2.1 m tall. The still waterplane was defined at approximately 60% of the domain height. The model and flow field were symmetrical about the x-z plane at the model's centerline, so only half the width of the full domain was meshed. A symmetric boundary condition was then applied at this location.

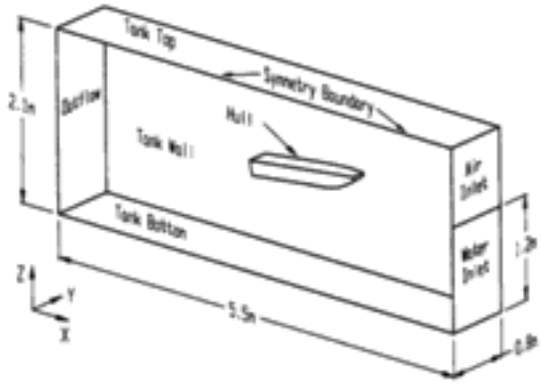

Figure 4: Planing Hull Model Domain

Another consequence of the small mesh size and the lack of turbulence modeling was that frictional resistance could not be predicted accurately. This problem was addressed by separating forces into pressure and frictional components. The numerical simulations provided the pressure forces while the frictional forces were determined by well-established empirical means (Lewis, 1988) as described below.

The wetted lengths of the numerical model were used to calculate the Reynolds number using the mean wetted lengths (Savitsky, 1964) as given by equations [1] and [2].

$$L_m = \frac{L_k + L_c}{2} \qquad [1]$$

$$Re = \frac{V \cdot L_m}{\nu} \qquad [2]$$

where,

L_m	is the mean wetted length
L_k	is the wetted length along the centerline
L_c	is the wetted length along the chine
Re	is the Reynolds number
V	is the model speed
ν	is the kinematic viscosity of water

The Reynolds number was used with the Schoenherr friction line (1947 ATTC Line), given by equation [3], to determine the coefficient of friction. The frictional force was calculated by equation[4].

$$\frac{0.242}{C_F} = \log_{10}(Re \cdot C_F) \qquad [3]$$

$$F_F = \tfrac{1}{2} \cdot \rho \cdot A_w \cdot V^2 \cdot C_F \qquad [4]$$

where,

C_F	is the coefficient of friction
F_F	is the frictional force on the hull
A_w	is the wetted surface area of the hull
ρ	is the density of water

Though only meant for fixed geometries, the CFD code was used to solve for the geometry-dependent problem of planing hull flow by incorporating it into an iterative solution scheme. An external program was written which ran both the meshing program (Gambit v1.2) and the solver, and evaluated the results from simulations. It executed the meshing program, adjusted the hull orientation, and then ran the solver. The results from the simulation were then evaluated and a new hull orientation chosen. This procedure is shown as a flow chart in Figure 5. In step (2) a journal file was a text file of commands for the meshing program Gambit. In step (3), a scheme file was another text file but with commands for the Fluent solver.

This method of using an external program to solve for equilibrium was found to work for the planing hull case, and can also be modified for a wide variety of problems in which the geometry of the domain and the flow field are inter-related.

The requirements for dynamic equilibrium for the planing hull evaluated in step (7) were that the net flow-induced vertical force must equal the weight of the model, and that the net trimming moment (taken about the tow point) from flow-induced forces must equal the trimming moment caused by the model's weight and center of gravity (also taken about the tow point). These two conditions specify the at-speed

resistance were instead attributed to an over-prediction of hull pressure forces.

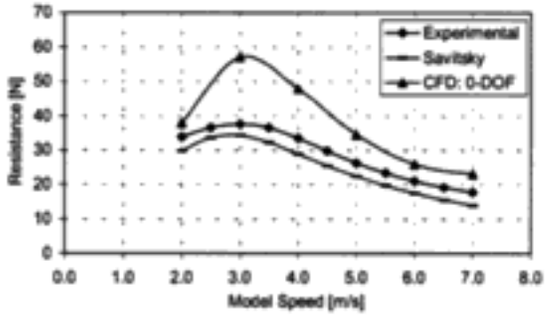

Figure 8: Pressure Resistance: 0-DOF

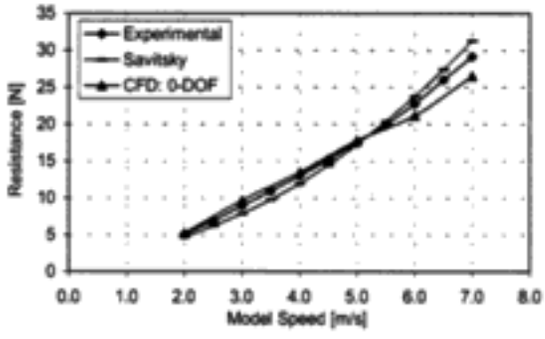

Figure 9: Frictional Resistance: 0-DOF

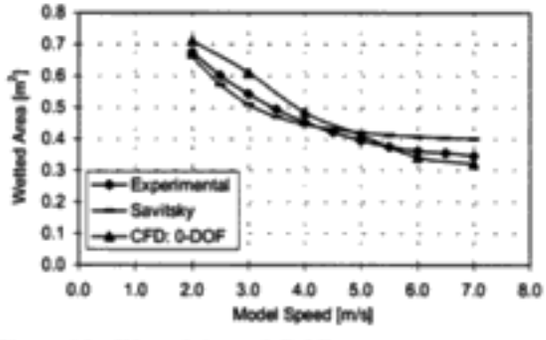

Figure 10: Wetted Area: 0-DOF

Several pressure taps were used in the physical experiments to determine hull pressures at speed. Comparing these results to the CFD simulations gave some indication as to where computed pressures were being over-predicted. Figure 11 shows the hull pressures measured during the physical experiments alongside those from CFD at the same locations. The four positions are labeled in terms of their distance from the transom measured parallel to the hull bottom. The 90mm and 530mm positions were on the centerline while the 620mm and 275mm positions were 50mm to the port side.

Experimental hull pressures near the stagnation region increased with increasing speed whereas the pressures near the transom showed decreasing trends with increasing model speed, even becoming negative at the highest speeds. The CFD results also followed these trends, although there were differences in the magnitudes when compared with the experimental values. The forward pressures seem to be under-predicted while the aft pressures were over-predicted. In other words, the pressure profiles indicated by the experimental results show considerably larger variation along the hull than produced by the CFD simulations. Generally, the region of over-predicted pressure (near the aft of the hull) was larger than the under-predicted region, which was isolated to near the leading edge of the air/water interface[2]. The net result of these higher than expected pressures led to an over-prediction of both drag and lift on the numerical model, despite a good correlation for wetted area and frictional resistance.

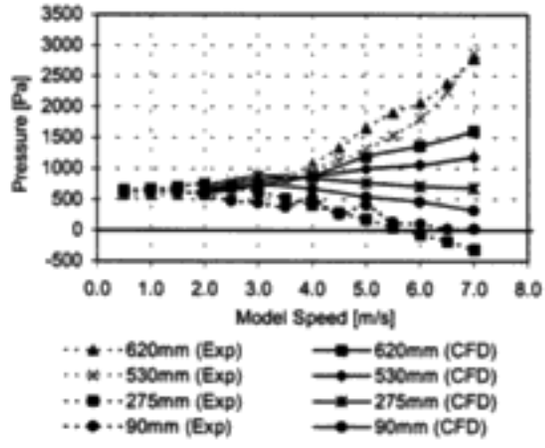

Figure 11: Hull Pressures

The hull pressures along the centerline of the hull are shown in Figure 12 for the CFD simulations. Given in terms of pressure coefficient (defined by equation [5]), several characteristics became apparent between model speeds. First, the wetted length was seen to decrease with increasing speed, as given by the locations of the peak pressures. The peak pressures, in terms of pressure coefficient, also decreased with increasing speed, although this was actually found to be a consequence of trim angle. The figure also shows the relative contributions to net lift

[2] The forward pressures were sensitive to the location of the leading edge due to a large pressure gradient near this region. Aft pressures were less sensitive due to a relatively smaller gradient.

sinkage and trim of the hull needed to properly determine resistance.

The behaviour of the forces and moments in response to changes in hull positions followed fairly linear trends (over a small range of sinkage and trim angles). This allowed for some interpolation of values, thereby saving computation time. Typically anywhere from 6 to 8 iterations were used to determine the equilibrium position of the hull per speed tested.

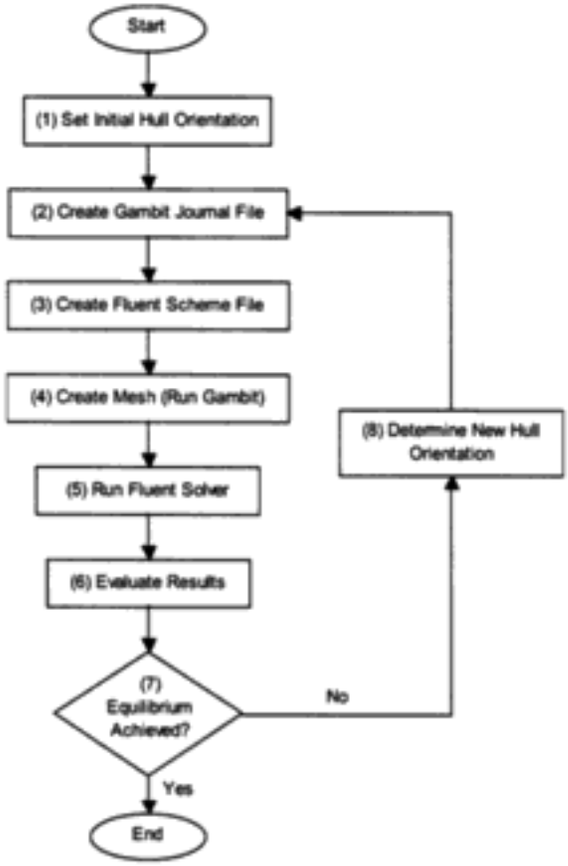

Figure 5: Flowchart for Equilibrium Program

0-DEGREE OF FREEDOM RESULTS

This section presents the results of CFD simulations where the orientation of the hull was set to match those determined from the physical experiments for each speed (shown in Figure 6). These tests were used to directly compare the experimental and computational results for the planing hull model.

In general, the CFD results for the 0-degree of freedom case were higher than those seen in the experimental results. Shown in Figure 7 are the total resistance curves for the experimental results, the CFD results, and those obtained by applying Savitsky's method (Savitsky, 1964). The results from Savitsky's method under predicted the experimental results, though at higher speeds the results tended to improve. The CFD results were above the experimental results, particularly in the 3.0 to 4.0 m/s range. Similar trends are seen in Figure 8, which shows only the component of resistance from pressure forces. Savitsky's method uniformly under predicts the experimental data, while the CFD results over predict the experiments. The worst comparison was at 3.0 m/s.

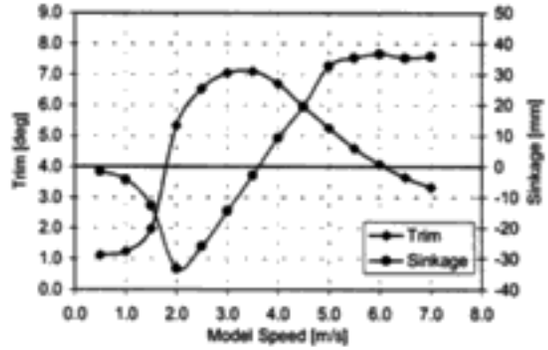

Figure 6: Experimental Sinkage[1] & Trim Results

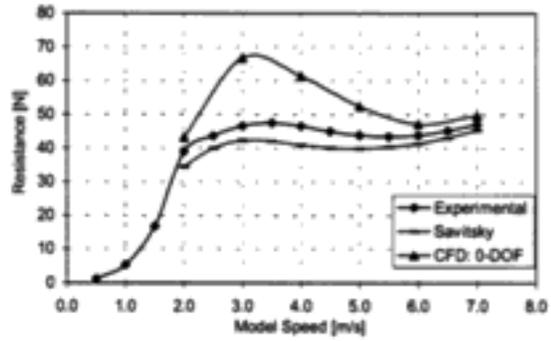

Figure 7: Total Resistance: 0-DOF

The frictional resistance results, shown in Figure 9, were well matched between the three sets of data. This was primarily a consequence of the similarly compliant wetted surface area results shown in Figure 10. Small deviations in the CFD results were likely due to experimental error in the determination of sinkage used to set the vertical position of the numerical model for these simulations. As these variations were small, they cannot account for the high values of total resistance. High values of

[1] The sinkage values given are the difference between the vertical positions of the tow point at speed to the tow point at rest. Positive values mean the tow point has risen.

from hydrostatic and dynamic forces. At the slower speeds, there was a pronounced hump in the aft region caused by hydrostatic pressure. As speed increased this hump gradually dissipated.

The coefficient of pressure, C_p, is defined as:

$$C_p = \frac{P}{\left(\frac{1}{2}\cdot\rho\cdot V^2\right)} \qquad [5]$$

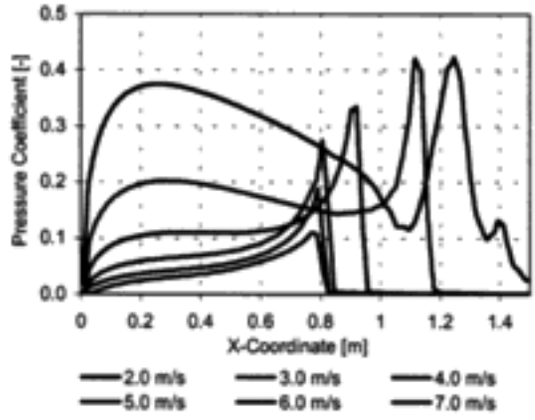

Figure 12: Pressure Distributions on Hull Centedine

The pressure profile for a CFD simulation of the model at 5.0 m/s forward speed is shown in Figure 13 as a pressure elevation plot. The pressure on the hull is represented as a 3D surface shaded by value. These results were consistent with some experimental data on prismatic hulls presented by Hirano et al. (1990), which gave a similar plot but based on physical model data.

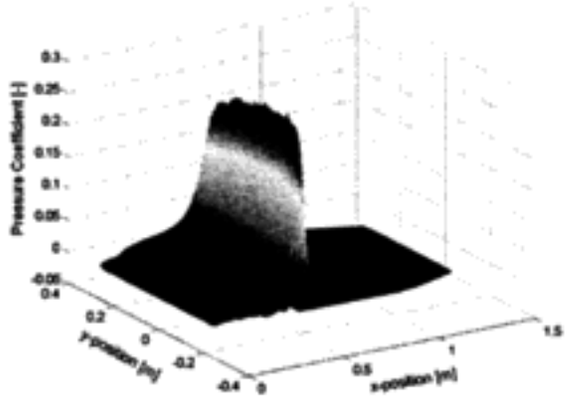

Figure 13. Hull Pressure (Model Speed = 5.0 m/s)

In order to better understand the differences between the numerical and experimental free stream velocities and pressures, their profiles along the centerline of the hull were examined. Figure 14 shows the total pressure from a typical CFD simulation along with experimental values. Also shown is the CFD velocity profile with experimental values (measured at two positions on the hull using a laser Doppler velocimeter). Velocities were taken at a position 15mm from the hull surface to ensure they were outside of the boundary layer.

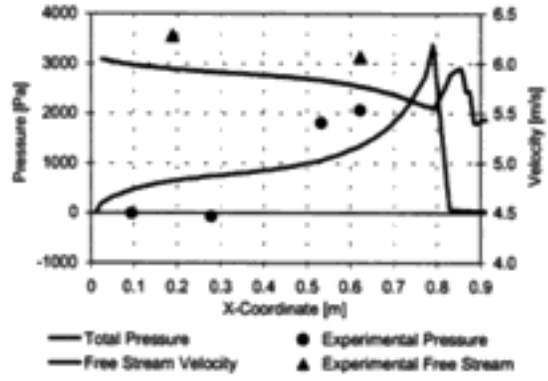

Figure 14: Pressure Profiles on Hull Centerline

These results were typical for this set of tests. Pressure was under predicted at the front of the hull and over predicted at the aft part of the hull. The apparent shift between the CFD results and LDV results from the physical experiments could be explained by a possible bias error in the physical measurement. However, the simulations significantly over predicted the net pressure force, suggesting that velocities were indeed being under predicted in the aft region.

The results from the zero degree of freedom simulations were found to follow the trends expected for a planing hull, although net pressure was over predicted. As net lift was higher than required for equilibrium, the next step was to balance net lift to the model's weight (in isolation of trim angle and trimming moment). This process is presented in the next section.

1–DEGREE OF FREEDOM RESULTS

In this set of tests, the model's vertical position relative to the waterline was altered by the equilibrium program so that net lift balanced the model's weight. The trim angle used for each speed was that measured during the physical experiments. The goal of these tests was to determine the sensitivity of the model to sinkage, and to establish whether deviations in the 0-degree of freedom model could be attributed to experimental error in this parameter.

location and magnitude of the resultant pressure force on the hull. As the location of this force was not relevant to the decomposition of the vector into lift and drag on a flat plate, altering the vertical position of the model was therefore equivalent to simply changing the magnitude of the resultant pressure force. The end result was that by requiring the lift component of this pressure force to equal the model weight[3], the drag force was inadvertently fixed to a value dependent only on the trim angle (given by equation [6]).

$$D_p = W_{Model} \cdot \tan(\tau) \qquad [6]$$

where,

D_p	is the pressure drag
W_{Model}	is the model weight
τ	is the trim angle

The drag force given by equation [6] is also shown in Figure 18 (labeled 'Pressure Vector'). There was a close match between both the experimental and numerical results to the theoretical values, particularly between 4.0 and 6.0 m/s. There were, however, discrepancies such as at 3.0 m/s. The numerical value was near the theoretical curve, but the experimental value was somewhat larger. The reason for this difference lies in the hull shape, and the difference in sinkage values for the numerical and experimental results.

As discussed, the CFD sinkage values were all somewhat larger than the experimental values, so that the CFD hull was relatively higher in the water. The numerical simulation at 3.0 m/s had a water contact area that still satisfied the 'flat plate' model and therefore had a pressure drag matching the theoretical value. In the physical experiments at this speed, the model was slightly lower in the water and the contact area included a region of the hull that began sloping upward towards the bow. This changed how the resultant pressure force was decomposed into lift and drag components. An illustration of this effect is shown in Figure 19. Part A) in the figure shows the flat plate case, while part B) simplifies the curved hull case with two flat plates at different angles. Although the net lift for the two cases is identical, case B) has a slightly larger drag value.

The differences in contact area between the experimental and numerical simulations are best described in terms of the length of the wetted centerline. These lengths denote the maximum distance that the wetted surface area extended forward on the hull bottom. Shown in Figure 20, the wetted lengths for both the CFD and experimental tests are presented. Also shown in the figure is a line designating the point at which the hull begins to curve upward towards the bow. Points below this line followed the flat plate model and had pressure drag measurements matching the theoretical values. Points above this line tended to have higher pressure-drag values than given by equation [6].

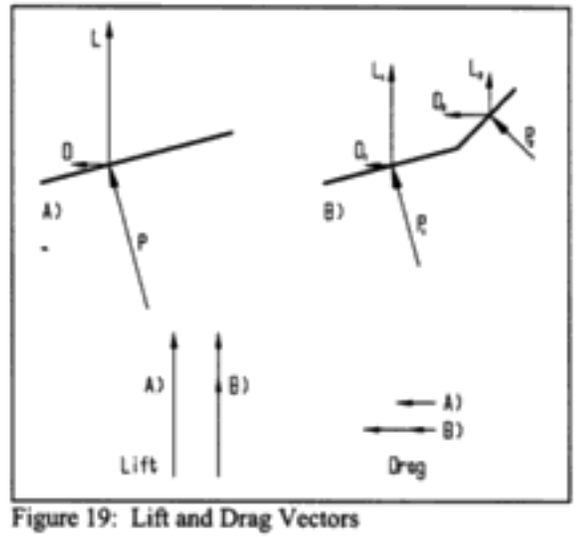

Figure 19: Lift and Drag Vectors

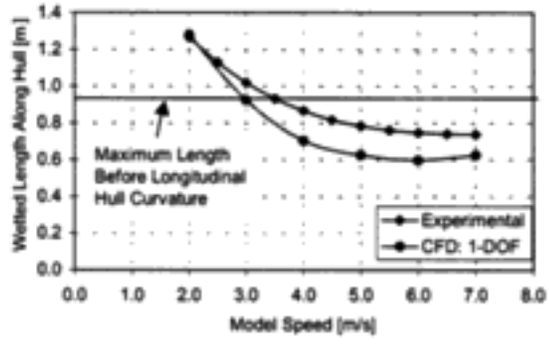

Figure 20: Wetted Centerline Length: 1-DOF

The results from this set of simulations led to the following conclusions. They show that by removing the frictional drag (calculated by the method discussed) from the total measured drag, the resulting pressure drag falls on the curve predicted by simple theory, thereby validating the force component

[3] The constraint was actually that the net lift on the hull was equal to model weight; however, the contribution to net lift from frictional forces was in all cases less than 1%.

The resistance curves for the CFD runs, the experimental tests, and Savitsky's method are presented in Figure 15. The hump speed, hollow and resistance increase were all clearly followed by the CFD predictions, showing some improvement over the Savitsky results.

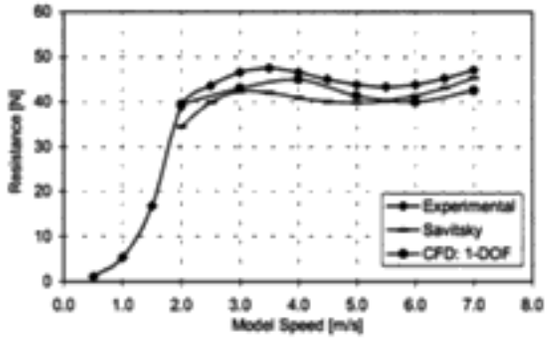

Figure 15: Total Resistance: 1-DOF

The frictional resistance, shown in Figure 16, was lower than the experimental values. This was primarily a function of the wetted area, which followed a similar trend. The low wetted area results were attributed to the fact that the final sinkage values for the simulations that satisfied the 1-degree of freedom equilibrium condition were higher than those measured during the physical experiments. Shown in Figure 17, the sinkage values for both the CFD and experimental results are given. The numerical model was farther out of the water than the physical model, thereby having less hull submerged and therefore less wetted area. This confirmed that the pressure forces calculated by the numerical method were greater than those produced by the actual flow.

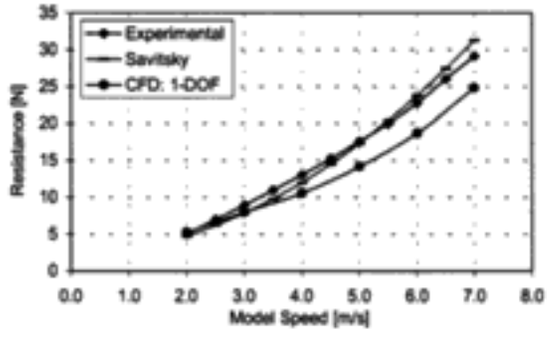

Figure 16: Frictional Resistance: 1-DOF

Figure 18 shows the pressure resistance for the numerical, experimental and Savitsky results. The pressure resistance was computed for the experimental results by first calculating the frictional component, and then subtracting that value from the total measured resistance. The numerical pressure resistance was computed by directly integrating the pressure forces over the hull area. The results for the 1-degree of freedom CFD simulations closely match those from the experimental results, despite the differences in sinkage, wetted area and fictional resistance. This match was attributed to a combination of the nature of the 1-degree of freedom constraint, and the shape of the hull.

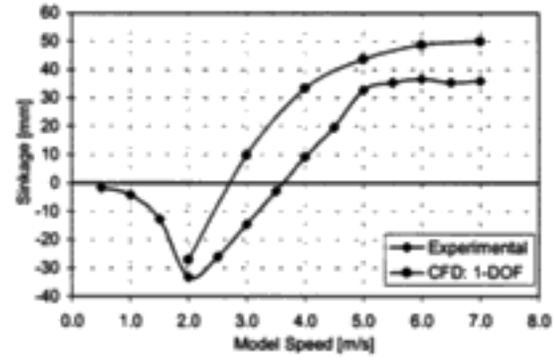

Figure 17: Sinkage: 1-DOF

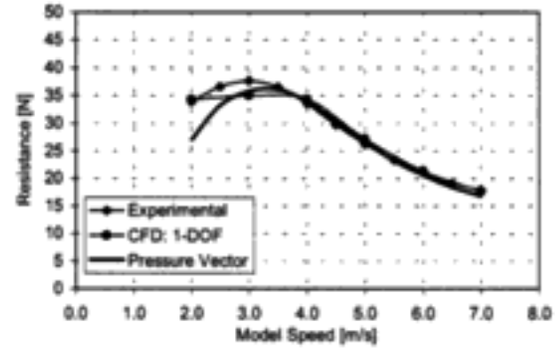

Figure 18: Pressure Resistance: 1-DOF

The 1-degree of freedom simulations required that the net lift (vertical force) exerted on the model was equal to the model's weight. When planing at high speeds, the portion of the hull in contact with the water was essentially planar in the longitudinal direction. This and the fact that the transom was dry meant that the system could be crudely represented as a flat plate with a pressure force acting perpendicular to it. This force can be expressed as a vertical component (lift) and a horizontal component (drag), whose magnitudes depend on the size of the pressure force and the trim angle of the plate (see part A in Figure 19). In a 1-degree of freedom simulation, the trim angle was held constant while the vertical position of the hull was altered, thus changing the

separation procedure[4]. This also supports the use of the method for the CFD case, which can result in large savings in mesh size and computation time. The 1-degree of freedom CFD results match the curve from simple theory, showing that the equilibrium solving procedure was working properly. The high values of sinkage and low values of wetted area for the CFD results compared with the physical experiments show that net pressure was being over predicted. Examination of the flow field in the CFD simulations suggested that the pressures on the hull were higher in the aft region and lower near the air/water interface than the experimental measurements. Free stream velocities followed the experimental trends, but were offset to lower values. In general, the computed flow was qualitatively consistent with experimental observations of planing hull flow, but actual values tended to deviate from the physical data.

2–DEGREES OF FREEDOM RESULTS

The last set of simulations involved solving for dynamic equilibrium of the steady state motion of a planing hull through calm water. Both sinkage and trim values were used to determine the model orientation for which the net vertical force and net trimming moment on the hull were zero.

The results from this set of simulations generally under predicted those of the physical experiments, except for sinkage, which was over predicted. These trends were consistent with excessive surface pressure forces computed for the planing hull. As discussed for the 1-degree of freedom case, the CFD hull was lifted higher than expected to balance the model's weight at the experimental trim angle. The resulting decrease in wetted area not only produced low values of frictional drag, but also shifted the location of the net pressure force farther aft. Due to a smaller 'moment arm' the net trimming influence on the model was also substantially reduced.

As the magnitude of net pressure force was effectively fixed by the lift equilibrium requirement, the only alternative left to increase the trimming moment was to shift its location forward. This was achieved by lowering the running trim angle. Other consequences of this move were an increase in wetted area, and hence frictional drag, a decrease in sinkage, and a decrease in pressure drag.

[4] In fact, provided the water contact area is within the portion of the hull without longitudinal curvature and the transom is dry, the frictional component of drag could be determined simply by subtracting the theoretical pressure drag from the measured total drag.

The results for running trim and sinkage are shown in Figure 21 and Figure 22 respectively. The trends were roughly followed, though there were shifts in the relative locations of the curves on the plots. The trim angles were all uniformly lower and the peak was shifted from approximately 3.2 m/s to between to 2.0 m/s and 3.0 m/s. Sinkage values were improved slightly from the 1-degree of freedom model but were still higher than the experimental values.

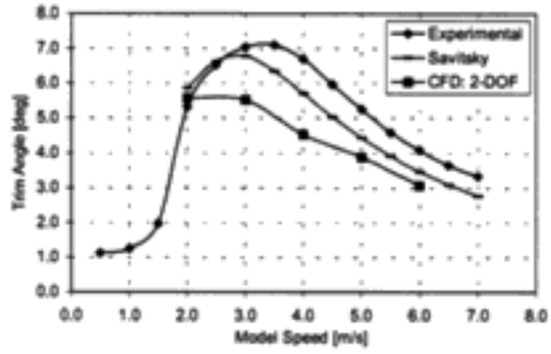

Figure 21: Running Trim: 2-DOF

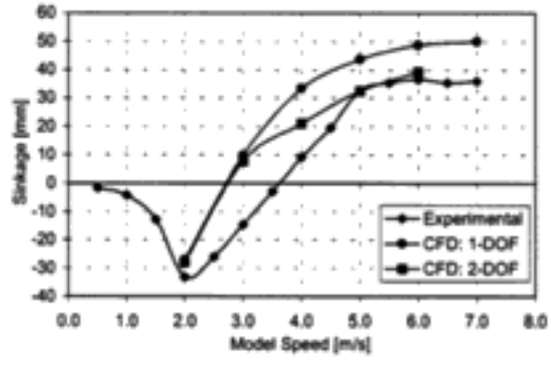

Figure 22: Sinkage: 2-DOF

Figure 23 gives an illustration of typical model orientations for the three sets of simulations that were performed. The top hull has a trim and sinkage corresponding to the experimental measurements, or the 0-degree of freedom model. The second hull has the same trim angle but has been lifted higher out of the water and represents the 1-degree of freedom model. The last hull shows the 2-degree of freedom orientation, lower in the water than the second hull and with a smaller trim angle.

In general, the wetted lengths followed the pattern shown in the figure. The 2-degree of freedom orientations had larger wetted lengths than the experimental values even though they had matching vertical forces and trimming moments. This increase in length was attributed to the fact that the net

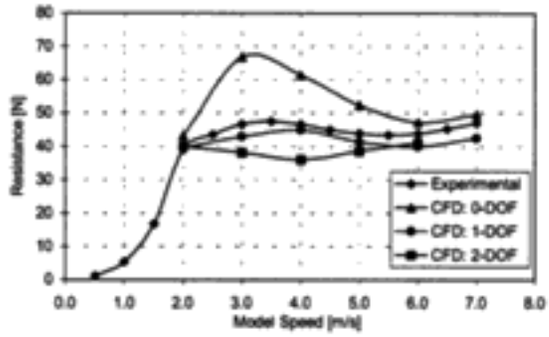

Figure 27: Total Resistance: 2-DOF

CONCLUSIONS

Predicting the performance of a planing hull requires the solution of dynamic equilibrium. It is through balancing lift and trimming moment with the model's weight and center of gravity that the proper trim angle and sinkage are determined. These parameters are essential for an accurate prediction of resistance. The goal of this project was to extend the ability of a commercial CFD package to handle this type of calculation, thereby making it a versatile tool for estimating planing hull performance.

The first step was to evaluate the CFD method in direct comparison with physical experimental data. The results of this test showed that velocities and pressure profiles were in qualitative agreement with experimental observations. However, there was an over prediction of net pressure leading to higher lift and drag values (by as much as 20 N). The numerical model was then tested in a 1-degree of freedom (in vertical position only) system in order to balance the lift forces with the model's weight. The pressure drag improved to within 5% of the experimental values, although this did lead to a smaller wetted area and hence an under predicted frictional resistance by up to 10%. In simulations involving full dynamic equilibrium, trim angle was found to decrease as much as 2° in order to balance the trimming moment while simultaneously satisfying the lift requirement. This increased the wetted area but decreased the pressure drag, leading to low total resistance results.

All of the CFD results followed trends characteristic of a planing hull. However, for each set of tests, the curves were shifted or stretched in reaction to the requirements of each case, in response to high net computed values of pressure. For both cases of dynamic equilibrium (1-degree of freedom and 2-degrees of freedom), these high hull pressures led to low total resistance values. This result may be counter-intuitive, but was a consequence of the model's ability to change its orientation in response to the flow field.

The cause of the relatively high pressures in the CFD simulations was not determined. They could be caused by insufficient grid resolution, a common problem in numerical approaches. A grid dependence study was conducted, but did not investigate the effects of large element count increases (on the order of 10 times or more than those used here). Another possible contributing factor was the lack of turbulence modeling in these tests. Proper turbulence simulation could alter the character of the pressure profiles and lower the net pressure. The treatment of spray was also a possible contributing factor. Although the VOF free surface capturing method does allow for fluid to be ejected from the near hull above the free surface, it was not necessarily equivalent to the spray produced in the physical experiments. This phenomena may need to be modeled in future simulations. Despite the high pressure values, the results of these predictions were valuable and the procedure for solving dynamic equilibrium was proven to be successful.

ACKNOWLEDGEMENTS

These experiments were performed at the National Research Council of Canada's Institute for Marine Dynamics (NRC/IMD). In addition to NRC/IMD, funding and technical assistance was provided by Memorial University of Newfoundland, Oceanic Consulting Corporation, and NSERC (Natural Sciences and Engineering Research Council). Fluent v5.3 was made available through an educational research license from Fluent Incorporated.

NRC/ Institute for Marine Dynamics
http://www.nrc.ca/imd/
Memorial University of Newfoundland
http://www.engr.mun.ca/
Ocean Engineering Research Centre
http://www.engr.mun.ca/OERC/
Oceanic Consulting Corporation
http://www.oceaniccorp.com/
NSERC
http://www.nserc.ca/

REFERENCES

Brizzolara S., Bruzzone D., Cassella P., Scamardella A., Zotti I., "Wave Resistance and Wave Patterns for High-Speed Crafts; Validation of Numerical Results by Model Test",1998.

Du Cane P., High Speed Small Craft 3rd Ed. Temple Press Books, London. 1964.

pressure force did not shift proportionately with the wetted length. The pressure distributions changed with trim angle resulting in lower peak values for lower trim angles. Shown in Figure 24 is a plot of peak pressure values against trim angles for various 2-DOF simulations. A clear linear relationship is seen which was not speed dependent (e.g. runs were performed at 4.0 m/s and 5.0 m/s at approximately 5.2° trim, both simulations had essentially the same peak pressures coefficients). Experimental values presented by Hirano et al. (1998) also fit on this curve. They tested prismatic hulls at various speeds, all at a trim angle of 6.0° and measured peak pressures coefficients between 0.3 and 0.4.

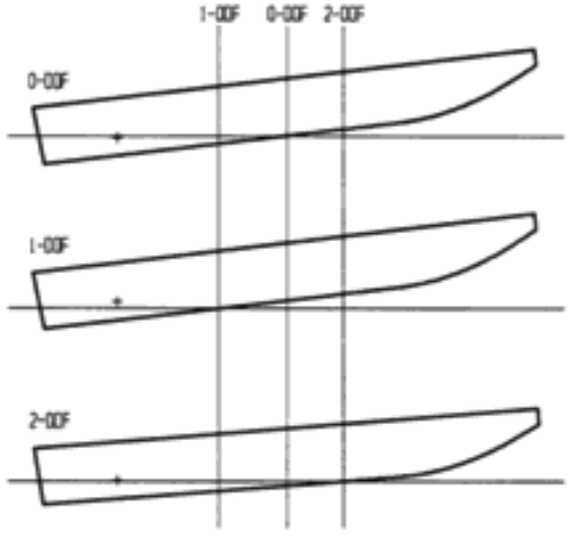

Figure 23: Hull Orientations

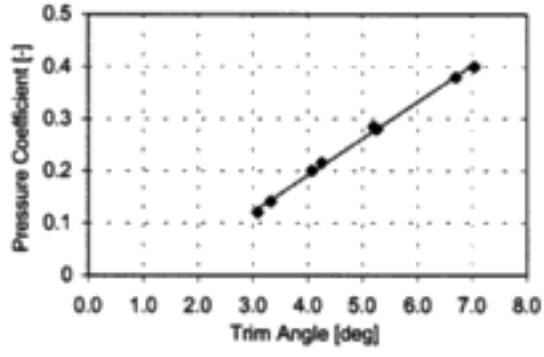

Figure 24: Peak Pressure vs. Trim Angle

The increased wetted lengths illustrated in Figure 23 also led to larger wetted areas. Whereas the 1-degree of freedom simulations under predicted wetted area, the 2-degree of freedom showed a slight over prediction as shown in the frictional drag results in Figure 25.

Pressure resistance values were lower in the 2-degree of freedom simulations, a direct consequence of smaller trim angles. They were, however, still in agreement with theoretical values calculated with equation [6] (using the new trim angles), provided the wetted lengths supported the flat plate assumption (Figure 19). The reduction in values, shown in Figure 26, demonstrates the importance of trim angle when predicting planing vessel performance. The results for total resistance are shown in Figure 27. The improvement in frictional resistance was not enough to counter the reduced pressure drag. The total resistance curve for the 2-degree of freedom system was therefore shifted downwards by as much as 10 N from the experimental one. The hump and hollow portions of the curve were also shifted about 1 m/s towards slower speeds.

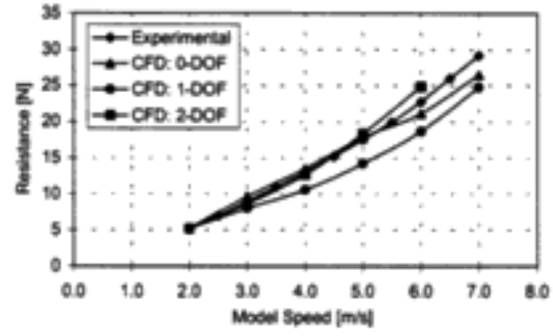

Figure 25: Frictional Resistance: 2-DOF

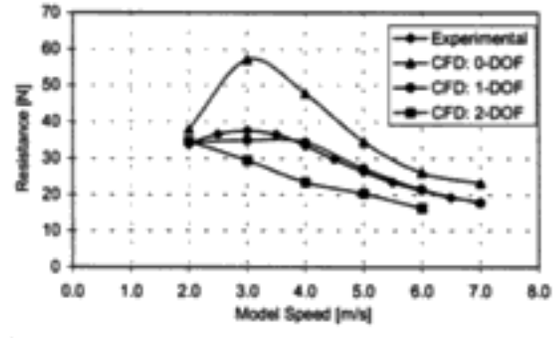

Figure 26: Pressure Resistance: 2-DOF

Hirano S., Uchido S., Himeno Y., "Pressure Measurement on the Bottom of Prismatic Hulls", Kansai Soc. Nav. Arch. J., No.213, March 1990.

Ikeda Y., Yokomizo K., Hamasaki J., Umeda N., Katayama T., "Simulation of Running Attitude and Resistance of a High Speed Craft Using a Database of Hydrodynamic Forces Obtained by Fully Captive Model Experiments", FAST '93, 2nd International Conference on Fast Sea Transportation, 1993.

Lewis E.V (ed.), Principles of Naval Architecture Second Revision, Society of Naval Architects and Marine Engineers (SNAME), Jersey City, 1988.

Löhner R., Yang C., Oñate E., "Viscous Free Surface Hydrodynamics Using Unstructured Grids", 22nd Symp. on Naval Hydrodynamics, Washington DC, pp. 128-142, August 9-14, 1998.

Payne P.R., Design of High Speed Boats Volume 1: Planing, Fishergate Inc. Annapolis. 1988.

Savitsky D., "Hydrodynamic Design of Planing Hulls", Marine Technology, vol. 1, no. 1, pp. 71 – 95, October 1964.

Subramani A.K., Paterson E.G., Stern F., "CFD Calculation of Sinkage and Trim", J. Ship Research, vol. 44, no. 1, pp.59-82, March 2000.

Thornhill, E. "Application of a General CFD Code to Planing Craft Performance", Thesis submitted to Faculty of Engineering and Applied Science, Memorial University, 2002.

Thornhill E., Veitch B., Bose N., "Dynamic Instability of a High Speed Planing Boat Model". Marine Technology, July 2000.

Yang C., Löhner R., Noblesse F., Huang T.T., "Calculation of Ship Sinkage and Trim Using Unstructured Grids". ECCOMAS 2000, 11-14 September 2000, Barcelona.

DISCUSSION

L. J. Doctors
The University of New South Wales, Australia

At the leading edge of the wetted surface of a planning hull (just behind the spray root), one has a stagnation region. Since the elevation of this point is very small (relative to the undisturbed free surface), one should realize a pressure coefficient of unity at all speeds.

Your results display a pressure coefficient much less than unity (0.1 to 0.4). Could you please comment?

AUTHORS' REPLY

The peak pressure coefficients in the CFD simulations were indeed well below the theoretical value of 1.0 predicted by classical planing theory (e.g. Du Cane 1964). Peak pressures were not measured during the physical experiments of this model for comparison. However, measurements of the pressure distribution (including the leading edge) on a planing hull model were conducted by Hirano *et al.* (1990). The peak pressure coefficients measured in these experiments were in the range of 0.3 - 0.4 putting them much closer to our computed values than the theoretical value of 1.0. It was also determined in our study that the CFD simulations were over predicting the net pressure force on the hull, which contradicts the premise that the computed pressures were too low.

Another consideration was raised when the computed peak pressure coefficients, though independent of speed, were found to be dependent on trim angle as shown in Figure 24. In planing theory the peak pressure would be 1.0 regardless of trim angle. This means that the peak pressure would have to jump instantaneously from 0.0 (for a hull with zero trim angle) to 1.0 given even the slightest increase in trim. Such jumps are difficult for real flows.

The behaviour of the spray root region also differed somewhat from the theoretical predictions. In the CFD model there was no flow projected forward (relative to the model) as spray. In the physical experiments, only a small trickle of water preceded the leading edge, the vast majority of spray was directed aftwards and to the side away from the model. Classical theory suggests that a much more pronounced forward directed spray should be produced, particularly at the flat bottom portion of the hull's cross-section.

It is possible that a region on the hull with a pressure coefficient of 1.0 did exist, but that it was so small and that the pressure gradient on each side was so steep that it could not be resolved by either physical experiments (for example, those done by Hirano *et al.*, 1990) or by the current numerical predictions. However, the above observations lead to the alternate conclusion that planing theory based on a 2D flat plate is insufficient to describe the flow around a realistic 3D planing hull form.

DISCUSSION

Hoyte C. Raven
MARIN, The Netherlands

From your Figure 1, the hull form appears to be very flat. Therefore, a smooth bow wave will not exist, spray/breaking/jet formation will occur at the intersection, and I suppose your choice for a VOF method may well be appropriate. To get an idea of how the method is performing in this area, can you show us what the computed bow wave and wave pattern look like?

AUTHORS' REPLY

Thank you for your discussion. As requested, here are a few examples of the computed free surface.

Figure 28 shows the free surface on the centerline plane (symmetry plane) of the model. The transom was dry as a gently sloping wave was produced behind the model. Free surface contours at elevations of ±15mm at 5mm increments are shown in Figure 29. The stern wave is shown as well as the beginnings of the system of divergent waves. These results are qualitatively in agreement with the waves observed during the physical experiments, which are shown in Figure 30 (coloured by elevation of the surface, blue represents the lowest levels, red represents the highest).

The air/water interface on the hull, which designates the wetted surface area, wetted centerline length and wetted chine length, is shown in Figure 31. The shape and contact area

closely matched those from the physical experiments. An image from the underwater video of the physical model experiments is given in Figure 32.

Figure 28: Free Surface at Centerline Plane

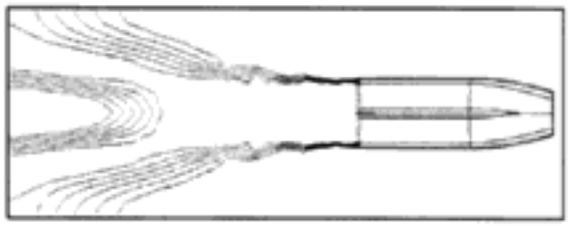

Figure 29: Free Surface Contours

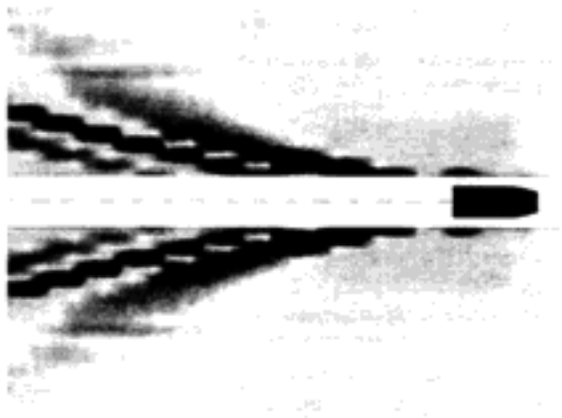

Figure 30: Wave Profiles from Physical Experiments

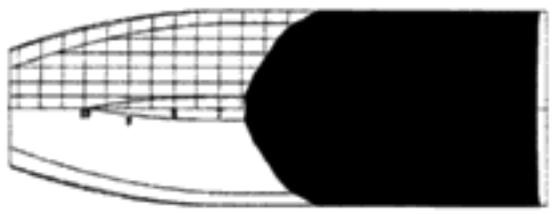

Figure 31: Wetted Surface Area from CFD

Figure 32: Wetted Surface Area from Experiments